2021

A COMPREHENSIVE FORENSIC CASE REPORT FOR THE BONNER COUNTY CORONER CASE #20-100

Megan Copeland
University of Montana

A COMPREHENSIVE FORENSIC CASE REPORT FOR THE BONNER COUNTY CORONER CASE #20-100

By

MEGAN CHEYENNE COPELAND

Bachelor of Science, Texas State University, San Marcos, TX, 2020
Bachelor of Arts, Texas State University, San Marcos, TX, 2020

Professional Paper

presented in partial fulfillment of the requirements
for the degree of

Master of Arts
in Anthropology, Forensic Anthropology

The University of Montana
Missoula, MT

December 2021

Approved by:

Scott Whittenburg, Dean of The Graduate School
Graduate School

Dr. Randall R. Skelton, Chair
Department of Anthropology

Dr. Katherine Baca
Department of Anthropology

Dr. Meradeth Snow
Department of Anthropology

Dr. Mark Heirigs
Department of Sociology

Copeland, Megan, M.A., Autumn 2021 Anthropology

A Comprehensive Forensic Case Report for the Bonner County Coroners Office Case #20-100

Chairperson: Dr. Randall R. Skelton

Abstract

This report consists of an inventory of the skeletal remains of case #20-100, assessment of the minimum number of individuals (MNI), a biological profile if possible, and a literature review of the use of DNA in ancestry estimations. The skeletal remains are consistent with an MNI of one. The remains are likely from a male individual, and skeletal features display a mixture of European and Asian characteristics. The individual is estimated to be between of 25-35 years old with an estimated stature of between 5’1” and 5’6”.

Background

On October 8, 2020, the Bonner County, Idaho coroner received a set of skeletal remains which were articulated with wires and other hardware, indicating it was likely an anatomical specimen (Photo 1). The remains were used by the Fraternal Order of the Eagles in initiation ceremonies. According to a previous member of the Eagles, once the remains were no longer being used in these ceremonies, the skeleton was placed in a box and stored in a garage until eventually being handed over to Coffelt Funeral Services for burial. The funeral home then turned custody of the remains over to the Bonner County coroner. The historical information of the remains reported by the Eagles members appear to have been based on local legends rather than documented facts.

Introduction

On Saturday March 13th, the remains were transported to the University of Montana for forensic analysis. Analysis of the case was assigned to Forensic Anthropology Masters Student Megan Copeland, BA, BS. The remains were stored in room 250A of the University of Montana Forensic Anthropology Lab (UMFAL), which is only accessible to individuals who are approved to participate in forensic analysis of state cases. For this project, a comprehensive forensic analysis was performed on case #20-100 to provide any information possible regarding the identity of the remains before burial. Upon completion of analyses and the defense of this paper, the skeletal remains will be returned to the Bonner County coroner.

Forensic analysis for this case includes the following: estimation of biological sex, age, ancestry, stature, pathology, and trauma. Prior to the assessment of these areas, a skeletal

inventory was performed, general observations were noted, and the remains were disarticulated to the most extent possible to better enable examination of different skeletal markers.

Case #20-100 consists of an articulated skeleton with the upper limbs separated from the scapulae and the lower limbs separated from the ossa coxae. Cartilage is present connecting the ribs to the sternum (Photo 2). The remains are mostly complete with only three missing elements: left 5th distal foot phalanx, right 4th distal foot phalanx, and the hyoid. All cranial elements (not including dentition) are present and complete. The dentition is not complete, and nine teeth are absent: 5, 8-12, 22, 27, and 28 (Figure 1). Maxillary and mandibular 3rd molars are not included in this count since they appear to be congenitally missing. Post-cranial elements are all complete apart from the ischial portions of the ossa coxae. The ischial tuberosities are missing from both sides (Photo 3 and 4). Cranial and post-cranial elements are in fair condition with varying degrees of post-mortem wear that can be attributed to its use as an anatomical specimen.

For ease of examination of skeletal markers, the remains were disarticulated (Photo 5). The process of disarticulating the remains was accomplished using a variety of wire cutters and screw drivers. The spinal column was articulated by nailing padding on the superior surface of each vertebra and placing them on a metal rod that was affixed to the sacrum. Upon removing the rod, the vertebrae were soaked in water for 30 seconds to remove the padding and nails. Fibrous padding was also present between the pubic symphyses. During disarticulation of this area, the posterior wall of the pubic symphyses were damaged (Photo 6). The ulnas and humeri could not easily be separated without damage to the bones and were left articulated (Photo7). The tibias and tali posed the same problem and were also left articulated (Photo 8).

Literature Review

Forensic Anthropology: The Biological Profile

Tracing back to Krogman's 1939 article in the Federal Bureau of Investigation Newsletter entitled "*A Guide to the Identification of Human Skeletal Material," anthropology has had a significant involvement with human remains in a forensic context (1,2).* Forensic anthropologists assist with the recovery and analysis of skeletonized humans remains, and as part of the analysis, a biological profile is constructed (3). The biological profile includes an estimation of biological sex, age, ancestry, and stature as well as analyses of trauma and pathologies. These estimations can facilitate an approximation of identification of victims in a forensic context or within archaeological remains (4). Although the biological profile can be helpful in aiding law enforcement with identification, problems and limitations exist with the methods used in constructing it.

Since the 2009 publication of the National Academy of Science's (NAS) report, "Strengthening Forensic Sciences in the United States: A Path Forward," research within the field of biological and forensic anthropology has spotlighted on validation studies of the commonly used methods in estimating the biological profile (5-9). The crux of the issue is that most of these methods are outdated, and/or the reference samples that the methods are based upon are not comparable to modern forensic remains. The most accurate age estimation methods rely on dental eruption and dental attrition (10). Yet, the main methods assessing these factors rely on reference samples of a specific ancestry that range in antiquity from historic to pre-historic (11,12).

Specific ancestry and antiquity-based methods become problematic when the skeletal remains in question do not belong to the specified reference groups. This can lead to results becoming distorted. Antiquity in particular has become an increasing issue with these methods because recent studies have shown that secular change has occurred at a faster rate than previously believed (13). Within the last two centuries in the United States and other industrialized countries, secular changes have been recorded for stature, weight, body proportions, and skeletal maturation rates (14). Technological advancements have led to a sedentary lifestyle and better nutrition and overall health have greatly influenced the skeleton's biomechanical structure (15). One study showed a significant decrease in mediolateral diameter of the femoral midshaft, which was associated with a decrease in physical activity (14). Furthermore, human development has also been affected by these lifestyle changes. Studies comparing modern children to children from historic eras have shown a significant difference in the progression through pubertal stages (16). Therefore, as evident by these studies on secular change, methods based on historic samples and earlier cannot be accurately applied to samples of modern context.

Even Fordisc, a program renowned as a powerful tool in metric age, ancestry, and stature estimations, is limited by its reference samples. The program only has eight reference populations in the Forensic Anthropology Data Bank (FDB) for ancestry estimation, and only half of these have both male and female references available (17). While the Howells dataset includes more references populations (28 total), the measurements were obtained mostly from historic samples (Howells 1996). Stature estimation is even more limited with only African and White reference samples available (17). As a result of these limitations, several studies have been published criticizing the program (17-19). Two other studies, one of which focuses on persons of

European descent, even advises that morphological analysis should be used instead of Fordisc for individuals of certain ancestries until proper reference samples for said ancestries could be added to the program's database (20). Validation studies on these methods using remains of modern context and from various ethnic backgrounds would also provide a way to strengthen these methods. Texas State University and the University of New Mexico both own decently sized sample collections of modern contexts that would be suitable for this purpose.

Errors with Fordisc are more prominent in relation to ancestry estimations, especially when classifying remains of Hispanic descent. An article from 2019 attributes misclassifications of Hispanic descent to admixture (21). This brings forth another issue within anthropology: should ancestry estimations even be included in the biological profile? Ancestry is notorious within the field of biological anthropology for being difficult to assess (22). Due to admixture and individual variation, ancestry is a much more fluid attribute than the differences between biological males and females, and this fluidity is in part due to admixture (23). In comparison, the other three components of the biological profile (age, sex, and height) are relatively fixed attributes, so the estimations for these categories rely on less ambiguous traits (24). In addition, ancestry estimations have gained notoriety in articles due to misconceptions of ancestry versus race (25). Ancestry in anthropology is defined as the geographic region or ancestral origin of a person, and race is a socially constructed category (22). Although forensic anthropology teaches and emphasizes this difference by strictly using the term "ancestry," many researchers argue that ancestry estimations still create an opening for of engaging in "phenotypic othering" (26).

This phenotypic othering can occur in part due to the difference in terminology and its implications as used by forensic experts, law enforcement, and lay people. Anthropologists can estimate ancestry, but this does not imply a direct correlation with skin color. So, even if the

estimated ancestry is African, this does not mean the individual is Black. Additionally, since these are only estimates, the results should not be viewed as absolutes because it can skew investigations (22,25,26). Despite efforts to distinguish ancestry and race from each other, misconceptions are still present in literature, forensic cases, and in conversation by the general public. A language study of the usage of "ancestry," "race," and "ethnicity" indicate that the general public use the three words interchangeably. "Ancestry" was used in the majority of forensic cases, but it was defined by law enforcement cultural, geographic, governmental, and/ or self-identity criteria, indicating that ancestry and race were still being viewed as the same. Interchangeable usage of these terms translates to a perpetual public misunderstanding which then causes a misrepresentation of forensic research (27). The difficulty of estimating ancestry combined with society's misunderstanding of ancestry versus race begs the question of whether ancestry should continue to be included within the biological profile. Many argue that, because ancestry estimates have the possibility of hindering identification, it is counterproductive and should not be used (26). The latest rebuttal to this argument states that it should be reported but not used by itself. Ancestry estimates based on the skeletal remains should be combined with other methods such as genetic analysis, and the caveats of these estimates need to be made abundantly clear to law enforcement and the general public (28, 29).

A similar problem is the divide between sex and gender. Forensic anthropologists are only able to provide estimations of an individual's biological sex (30). Since gender is a socially constructed categorization, forensic anthropologists' estimation of biological sex does not provide information to an individual's gender (31). Juvenile remains are shown to be another limitation of sex estimations. The traits commonly assessed for biological sex are still developing and remain ambiguous in juveniles until after puberty (32). Other problems arise from the

varying degree of sexual dimorphism between populations and the unknown effects of pregnancy on ossa coxae morphology (33). Sexually dimorphic traits are not as simple as whether the observed trait is present or not, but rather, these traits fall within a scale according to prominence/robusticity. The degree of ruggedness of these traits can be misperceived depending on the overall size of the individual. Individuals from Asia for example tend to have smaller builds, and this can make the skeleton seem more gracile than they actually are (34). To avoid this, sexually dimorphic traits should be considered relative to the size of the individual to determine prominence/robusticity, and since many sex estimation methods are visual assessments, interobserver error is another key issue (25). Furthermore, facial surgeries are now available for individuals who are transitioning as a way to better reflect their gender. Forensic anthropologists know little about the impact this will have on sex estimates, but preliminary studies suggest that these surgeries provide enough evidence to make inferences on gender. However, the majority of these surgeries are feminization surgeries, so this would not be able to be as widely applied to transgender men (female to male) (30).

MtDNA: Identification and Ancestry Estimation

Inherited solely from the maternal lineage, mitochondrial DNA (mtDNA) was first discovered by Margit and Sylvan Nass in the 1960's via electron microscopy (35). The mitochondrial genome spans approximately 16,500 base pairs and is passed onto offspring through the maternal lineage (36). Within the mitochondrial genome, 37 genes exist that code for 13 proteins, 22 tRNAs, and 2 rRNAs. The 13 proteins coded for all instruct cells to generate protein subunits of the enzyme complexes of the oxidative phosphorylation system, enabling the mitochondria to carry out its function as the powerhouse of our cells (37). The D-loop is a control region within the genome that is 1,122 base pair long, and it is the most polymorphic

region. This region can be divided into the Hypervariable region I (HVI) and Hypervariable Region II (HVII) (38).

The Cambridge Reference Sequence (CRS) was the first complete human mitochondrial genome to be sequenced. It was initially published in 1981 but has since been revised (39). Compared to nuclear DNA (nDNA), mtDNA is both more abundant and prone to mutation, and overall, mtDNA survives longer than nDNA due to its abundance. Thus, mtDNA is beneficial in cases where the sample DNA being sequenced is ancient or degraded due to the high number of copies (40).

Forensic research has spotlighted mtDNA sequencing because of these advantageous characteristics, and studies have shown that mtDNA sequencing is a robust method regarding cases of exclusion or absence of identity (36). Since the 1980s, mtDNA has become routinely used in forensic investigations, and it is considered the last resort for remains or samples that are highly degraded (41). In 1991, Stoneking et al. published the first report of mtDNA typing being successfully used in a forensic human identification case. The forensic lab was able to identify the skeletal remains of a child by using hybridization with 23 sequence-specific oligonucleotide probes targeting 9 regions of HVI and HVII on the control region. The resulting mtDNA type matched with the suspected mothers. The conclusions from this case lead to scientists to posit that mtDNA typing could have potential in sexual assault cases too (42).

Additionally, despite the successful identification in the aforementioned case, mtDNA analysis is still limited in the results it can provide because it only follows the maternal lineage. As such, mtDNA has a lower discrimination power when compared to nDNA, which becomes an issue in forensics when common mtDNA types are involved (36). For example, in Europeans, the most common HVI/HVII type is found in approximately 7% of the population (43). As a way

to increase the discrimination power, researchers have begun large scale sequencing of the entire mitochondrial genome of individuals with common HVI/HVII types (43, 44).

Data from mitochondrial DNA sequencing can not only be compared for matches but can also be used as an indicator of lineage. Phylogenetically related haplotypes are formed through the accumulation of variation (45). Beginning with "Mitochondrial Eve"- the most recent common ancestor matrilineally- four haplogroups (L0, L1, L2, L3) specific to sub-Saharan Africa split off and continued to branch out, forming sub-haplogroups (46). For example, the M and N lineages originated from the L3 haplogroup (47). These haplogroups continued to branch off as depicted in Figure 2, and the current mtDNA phylogenetic tree contains more than 4,000 haplogroups (48,49).

The different haplogroups can be categorized by the geographic region according to their frequency within those regions under the assumption that a high frequency in that area means that haplogroup likely originated there, but this is not always proven to true (37). With this assumption though, mitochondrial DNA can be sequenced and matched to a haplotype based on its specific single nucleotide polymorphisms (SNPs), and from that, the haplotype or overarching haplogroup can be used to infer maternal ancestry (50). For example, haplogroups J and U are regarded as part of the European haplogroups because of their high density in that region. The F haplogroup is predominately considered as an Asian haplogroup because it ranges from 31 to 77 percent in different parts across Asia (51). The inherent problem with this method in ancestry assessment is the underlying assumption described previously. Because populations continue to migrate and new mutations appear in these populations, the difficulty of locating the origin of a specific haplogroup or mutation increases (37). Therefore, inferences based upon the method should be considered with some caution.

Anatomical Specimens

Often found within schools and skeletal collections, anatomical specimens are deeply entangled with the sciences and biological anthropology, and one of the first records of anatomical studies using human remains trace back to the 5th century BCE (52). Use of human remains in science studies became more pervasive during the 17th century, and in France, the studied remains were often criminals who had been executed (53). Unlike France, anatomical specimens in America were not obtained from within the nation. Since America's mortuary practice timeline is short, meaning individuals are buried soon after death, the majority of anatomical specimens present in America originated overseas, and if they were used in studies, the remains usually ended up on a medical dissection table (54). Americans, due to their fear of death and the unknown, attempt to deny and defy death through their mortuary practices (55). Part of this is done by burying the decedent relatively quickly as stated above. On average, individuals are buried between three to five days after death (56). The other part of this can be seen through the prevalence of embalming in American mortuary culture. Embalming preserves the state of the body, and in a sense, disguises all the signs of death by delaying the decomposition process (57).

As a result of America's mortuary practice, anatomical specimens had to be outsourced, and a large percentage of these specimens were imported from India, which had been a leading producer of human remains throughout the 1970s (58). Since export of human remains was banned in India during the mid-1980s and China (another big leader in producing anatomical specimens) in 2008, American retailers have had to purchase the specimens from international third parties (54, 58). Unfortunately, many of these remains were obtained under unethical circumstances. A large portion of the medical specimens in India and those that were exported

from India were unclaimed bodies. Economic conditions and poor communication modalities caused a massive collection of unclaimed bodies in India, which the government allowed to be sold and exported. The number of unclaimed bodies has since declined due to the public outcry and multiple legislative initiatives being implemented (59).

Recently, activists have been raising attention to the vast amount of remains that had already been exported under these conditions and has led a call for the repatriation of these anatomical specimens (54, 58). On top of this, activists are also fighting for a reevaluation of the human bone trade (58). With the explosion of multiple social media platforms, new avenues for buying and selling human bones have appeared. In particular, TikTok user Jon Pichaya Ferry has been the center of controversy because of his collection of human bones. Jon Ferry sells these bones online under the claim that the bones he sells were all bones specifically prepared to be used as anatomical specimens (60). However, others have argued saying the origins of these remains are questionable at best and could have been initially obtained through unethical and/or illegal means (58). This could occur through situations like in India as previously described, grave robbing, or even murder. In 1828, William Burke and William Hare became infamous for having murdered sixteen people in order to sell the bodies to doctors as dissection specimens (61). While murder is not a common occurrence in this trade, these murders emphasize the potentially problematic history of anatomical specimens with unknown origins (49).

Applications to BCC #20-100

Case BCC #20-100 provides a key example of why the methods for constructing the biological profile should be strengthened as well as the importance of anatomical specimens and their origins. The remains in questions were prepped and used as an anatomical specimen. However, as mentioned, this does not mean that the individual consented to this prior to death.

Providing as much identity as feasible to the individual is one of the only options that can be done at this point. Reconstructing the identity of the deceased is a significant and serious task, so it is important that the methods used to do this are as stringent and widely applicable. Accuracy of these methods need to be determined via large, well-designed studies on individuals of varying backgrounds. In this case, the biological profile of case BCC #20-100 was constructed using the methods common in forensic anthropology. However, these methods are based on specific reference samples that do not match with the traits of this individual. Because of this, molecular analysis was used to strengthen the ancestry estimation but is limited to only the maternal ancestral lineage. The features of this case ties into multiple areas of study and their uses while also underscoring the key problems in these fields.

Materials and Methods

Sex

Sex estimation from the ossa coxae is widely known as having the highest accuracy largely due to the pivotal role of the pelvic girdle in childbirth, and as a result, the structure of the human pelvis has multiple sexually dimorphic features that can be used for sex estimation (63-65). Commonly observed features include the shape of the subpubic angle, presence of a ventral arc, width of the ischial-pubic ramus, angle of the greater sciatic notch, and shape of the preauricular sulcus (66-70). Two methods of sex estimation based on the sexually dimorphic features of the pelvis were conducted using the left os coxa. The Phenice (1969) and Klales et al. (2012) methods both focus on the pubic portion of the os coxa. The former is a visually based method while the later employs an ordinal scoring system and linear regression equation to estimate biological sex (66, 70).

Despite the persisting notion that the cranium is the second-best indicator of sex, multiple studies have determined that the majority of post-cranial markers are more accurate than the cranial based methods (71-74). As a manner of estimating sex utilizing post-cranial elements, the morphology of the distal humerus was examined using the Rogers (1999) method, which indicated a 92% accuracy of sex estimations when performed in the initial study. This manner of analysis focuses on three main traits of the distal humerus- the shape of the olecranon fossa, angle of the medial epicondyle, and trochlear extension (75).

Although post-cranial studies showing higher accuracy results, the cranium can also be used as an indicator for biological sex estimations with approximately a 70% accuracy (76). This can be especially useful in cases where the ossa coxae are not present or too damaged to be used (3, 77). A morphometric assessment of the skull was used to estimate sex based on five traits that are generally recognized as being sexually dimorphic: nuchal crest, mastoid processes, supraorbital margins, glabella, and mental eminence (78). This method scores each trait on a range of 1 to 5 using the Buikstra and Ubelaker (1994) scoring and uses a logistic regression equation to provide an overall percent probability for the estimated biological sex (78, 79).

Age

The ranges for age at time of death was estimated using a variety of methods based on cranial and post-cranial skeletal markers. Since epiphyses and sutures fuse at different stages during human development, they can be a highly reliable source of age estimation, particularly for juveniles (79-82). Moreover, even if a specified age range is unattainable, sutures can be used to establish whether the bones in question belonged to an adult or not, and based on that result, one can then choose the next most appropriate method for estimating age. In this case, two sutures were examined- the basilar suture (79) and medial clavicular epiphyses (83).

The use of dentition in age estimations is common practice, and, similar to epiphyseal fusion, it is especially accurate when working with subadult samples (12, 84). While dental eruption can help provide foundation for a minimum age estimate, dental attrition is more useful when working with adult samples (85). Maxillary and mandibular dental wear was assessed using the Brothwell (1981) and Lovejoy et al. (1985) methods (11, 12).

Sternal rib end analysis was utilized for the age-at-death estimation because it has been shown to be a highly accurate age assessor in skeletons of both sexes (86). According to Iscan et al. (1984), rib end characteristics such as pit shape and wall configurations are regarded as being more accurate than just using pit depth (87). It is cautioned that researchers and anthropologists consider that sternal rib ends can be influenced by biomechanical variation and sex and can therefore impact age estimations (87,88). Although research has suggested that sternal rib end analysis methods can be used on the third rib, the fourth rib was analyzed for this case using the revised descriptions within the Harnett (2010) study (6). Results were applied to ageing categories derived from the Maricopa Forensic Science Center (FSC) samples (Harnett 2010) and the Iscan et al. (1984) samples for males (6, 87).

Estimations using the pubic symphyses were not performed due to the surface of the symphyses being obscured by the padding that was glued on when the skeleton was re-articulated after death.

Ancestry

To estimate ancestry, mitochondrial DNA (mtDNA) analysis was executed using bone samples from the petrous portion of the right temporal bone by using a Dremel rotary tool to drill through the external auditory meatus (89). Drilling took place in room #237 over a sterilized

sheet of butcher paper inside a fume cabinet, and personal protective equipment (PPE) consisted of gloves that were sterilized with DNA Away, masks, and goggles. Approximately 0.082 grams of bone dust was collected into a weigh boat and placed in a 2 ml tube. All plastic consumables had been exposed to UV-C light to decontaminate surfaces for at least 15 minutes.

Extraction was performed using a modified version of the Dabney protocol (90). A negative control sample was prepped with the same procedures to test for contamination being introduced from lab reagents. One milliliter of EDTA was added to the extraction tubes to breakdown the samples, and the tubes was vortexed to ensure proper mixing. The samples were stored in a drawer overnight. Ten ul Proteinase K was added to the tube on the following day to lyse the cells. Following this, the samples were allowed to incubate with parafilm sealing the top to prevent leakage for approximately ~1 hour at 55 degrees Celsius to inactivate the Proteinase K. After incubation, samples were spun down in a centrifuge, and 1 ml of supernatant was transferred to a 15 ml tube with 13 ml of PB buffer (Qiagen). This mix was then placed in a Qiagen spin column and spun through a silica extraction filter. The DNA was bound to the silica membrane. Afterwards, two 700ml ethanol washes were performed to wash away any contaminants, and then a dry spin was done. Lastly, two more spins were done using 55 ul of double distilled water (ddH_2O) to elute the purified DNA. The DNA was quantified using a Qubit (ThermoFisher; 0.245ng/ul) before starting the library preparation protocol, which is the first step Next-Gen sequencing. Library preparation allows for the DNA to adhere to the flow cell and for the sample to be identified.

In Dr. Snow's aDNA lab at the University of Montana where the analysis was executed, a hybrid of the Meyer-Kircher (2010) and KAPA (Roche) protocols were used for library prep (91). A master mix (5ul NEBuffer2, 0.25 BSA, 0.5ul ATP, 0.6ul dNTPs, and 1ul

water per sample) for blunt-end repair was created. Once added to the samples along with 2ul T4 PNK and 2ul of T4 DNA Polymerase, the samples were incubated at 25 degrees Celsius for 30 minutes in the thermocycler since the DNA ligase enzyme reaches optimal activity at this temperature. A bead clean was performed, and the beads underwent two ethanol washes (70% ethanol). Next, 15ul of EB Buffer was added to each sample. Samples were loaded on a magnetic rack once again to remove the purified DNA solution. The solution transferred to new PCR tubes, and the DNA was resuspended in 18ul of EB.

To add adapters onto the DNA fragments, an adapter ligation master mix (14.8ul water, 8ul 5X rapid ligation buffer, 0.2ul annealed adaptors, and 2ul T4 DNA ligase per sample) was prepped, and 25ul of the mix was aliquoted into each PCR tube along with 15ul of blunt end repaired DNA. Samples were mixed gently and incubated for 5 minutes in the thermocycler at 22 degrees Celsius. Two bead cleans were performed. To fill in the single-stranded adapter sequences and complete the adapter annealing process, an adapter fill-in master mix (5ul ThermoPol Buffer, 0.6ul dNTPs, and 27.4ul water per samples) was created, and 40ul of this mix was transferred into each of the tubes. Adapter ligated, purified DNA (15ul) and *Bst* DNA Polymerase (2ul) were also added to each tube. Samples were mixed and incubated again at 37 degrees Celsius for 30 minutes and then at 80 degrees Celsius for 20 minutes.

Prior to another bead clean and to enable pooling of samples, 40ul of an indexing master mix (5ul ThermoPol Buffer, 0.5ul dNTPs, 1ul AmpliTaq Gold NDA Polymerase, 33.5ul water per sample) along with a P5 adapter (5ul), P7 adapter (5ul), and DNA from the adapter fill-in step (~50ul) were aliquoted into each tube. Following this, amplification of the sample library using LM-PCR began as described by KAPA. Thirty microliters of a Pre-Capture LM-PCR master mix was added to each sample. The PCR tubes containing the samples were then placed

in the thermocycler for amplification following the Pre-Capture LM-PCR program. The resulting amplified library was purified via a bead clean. Qubit was used again to quantify the DNA (52ng/ul).

Samples were then pooled along with aDNA samples from the Molecular Anthropology summer course during which this analysis occurred. After a bead clean, hybridization probes were added. Hybridization incubation occurred overnight at 95 degrees Celsius for 5 minutes then at 47 degrees Celsius for 20 hours. The DNA was captured using a bead wash. The beads with the bound DNA were washed using 40ul Stringent Buffer, 30ul Wash Buffer I, 20ul Wash Buffer II, 20ul Wash Buffer III, and 1000ul Bead Wash Buffer. The Post-Capture LM-PCR program was used to amplify the bead bound DNA. The samples were purified via a bead clean, and the DNA was quantified again.

Finally, samples were sequenced at the Genomics Core at the University of Montana using Illumina MiSeq Sequencing. Sequencing data was uploaded to a web-based bioinformatics platform (Galaxy)- using a pipeline created for Dr. Snow's aDNA lab. The raw data was inputted, and a FastOc was run to perform basic quality control checks. The pipeline then trimmed the adaptors and merged the forward and reverse reads. Next, the reads were mapped to a reference genome, and Qualimap generates data for read depth, sequence coverage, and the number of reads. Genotype calls then a consensus file are generated, and the overall sample contamination was estimated. The finished data analysis in Galaxy was entered into Haplogrep, a database that simplifies the process of identifying mitochondrial haplogroups by using pre-calculated phylogenetic weights that correspond to the occurrence per position in Phylotree (92). Results were organized and compiled into a spreadsheet.

In conjunction with the DNA analysis, non-metric and metric analyses were both used to estimate ancestry from the cranium. Non-metric cranial analysis includes a visual based method that uses a chart which classifies the different variants of a specific craniofacial trait into geographic races based on observed frequency (93). Additionally, another visual based method that uses a scoring system for the cranial traits was utilized (94). Based on the scores, the Hefner software will create probability matches for each ancestry. Ancestry based on craniometric data (Figure 3) was analyzed via the Fordisc 3.0 program (95). Cranial measurements were analyzed in Fordisc using the FDB dataset. The data was processed using all male populations available, and results were based on 21 measurements. Measurements with high deviations and were removed, and results were processed again. The input data was whittled down further to improve overall accuracy of the results by removing reference populations that were highly dissimilar.

Stature

Stature is a population dependent analysis, and since the individual for this case shows a mixture European and Asian characteristics, the Trotter (1970) method was utilized because it provides equations for both of these populations (96, 97). Equations for European and East Asian males were calculated using measurements from the radius, femur, and fibula. Certain measurements from the ulna and tibia were excluded because they could not be disarticulated without further damage to the bones. Therefore, accurate measurements could not be taken for these elements (Figure 4).

Although the Fordisc 3.0 program does not provide an Asian reference population for stature estimations, it does provide a European reference population. As such, Fordisc 3.0 was still used because the individual exhibits a mixture of characteristics. Stature was assessed using both European and African male reference populations using Trotter statistics to provide a more

inclusive estimate. Furthermore, a 95% confidence probability was used for these calculations. Once again, certain measurements were excluded from the ulna and tibia because the remains could not be fully articulated without further damaging the bones. Due to post-mortem damage, pelvic heigh and ischium length were excluded too.

Trauma and Pathology

The *Skeletal Trauma Analysis: Case Studies in Context* (98) was used to guide the observation and analysis of trauma for this case. For possible skeletal pathologies, the *Human Bone Manual* (99) and the *Identification of Pathological Conditions in Human Skeletal Remain* (100) were used as reference.

Biological Profile BCC #20-100

Sex

Os Pubis Dimorphic Traits

The Phenice (1969) method is a visual assessment of biological sex based on the sexually dimorphic features of the ventral arc, subpubic concavity, and medial aspect of the ischiopubic ramus (66). The os coxa exhibited the following: minimal presence of a ventral arc, little to no subpubic concavity, and a broad ischiopubic ramus with no distinct ridge. These features are most commonly observed in males, indicating the individual was male.

The Klales et al. (2012) method was developed to review and revise the Phenice (1969) method, and it provides a percent probability report for the estimated sex. The same three traits are used and are scored on a range from 1 to 5, with 1 being the extreme traits on the female side and 5 being the extreme for the male side of the spectrum (70). The ventral arc,

subpubic concavity, and medial aspect of the ischiopubic ramus each scored as a 4, indicating a 98% probability the individual was male (Figure 5).

Morphometric Skull Assessment

Out of the 5 traits examined for the Buikstra and Ubelaker (1994) method, the glabella/supraorbital ridges, mastoid processes, and nuchal crest all scored at a 3 (79). Both the mental eminence and orbital margins scored at a 4, exhibiting slightly more robusticity than the other features. These scores indicate with an averaged 82% probability the individual was a male (Figure 6).

Distal Humerus Morphology

The general shape of the olecranon fossa, angle of the medial epicondyle, and trochlear extension were employed as indicators for sex (75). For case #20-100, the individual presented olecranon fossae that were roughly triangular shaped. Additionally, the medial epicondyles were parallel or nearly parallel to a table's surface when held with the posterior end up, and the medial edge of the trochlea extended farther than that of the lateral edge. All 3 traits are most frequently observed in men, and as such, are indicative of that the individual was male (75). Results from each of the aforementioned methods indicate the individual was male.

Age

Suture Closure

The individual's basilar suture is completely fused, indicating a minimum age of 23 years (79). Likewise, the medial clavicular suture was also completely fused. This correlates with a minimum age also of 23 too according to samples retrieved from male U.S. military personnel

who died during the Korean War (83). Thus, it can be established that the individual was an adult at time of death.

Dentition

Dental attrition for case #20-100 was estimated in reference to the degree and patterns of wear as depicted in the dental attrition charts for Lovejoy et al, (1985) and Brothwell (1981). Maxillary dental attrition patterns aligned most closely with the phase E classification, correlating with an age range of 24 to 30 years of age (Photo 9). Furthermore, mandibular wear resembled that of phase G, which correlated to a slightly later age estimate of 35 to 40 years of age (12; Photo 10). The two estimates provide an overall age range of 24 to 40 years old; however, this method was developed based on samples from a pre-historic American Indian population from Libben, Ohio. Therefore, the population and antiquity of the samples for this method must be noted when taking these results into consideration.

To create a more inclusive and well-rounded age estimate, the Brothwell (1981) method was applied as well (11). Maxillary and mandibular molar wear patterns both matched best with a score of 3+ to 4. This has an associated age range of 25 to 35 years of age. It should be noted that this analysis is based solely on the first and second molars, and all the third molars were not included because they appear to be congenitally missing. As mentioned above, some discretion is advised regarding the age estimate results since this method is based on medieval English skeletons.

Sternal Rib End Analysis

The left and right rib ends both had shallow, V-shaped pits that did not show signs of billowing (Photo 11 and 12). The rims were smooth and round, without any scalloping or

irregular flaring. Minimal microporosity was present on the left rib pit. Rib end observations corresponded the best with the description for Phase 2. Phase 2 has an associated age range of 18 to 25 years based on the European rib end samples from the Iscan et al. (1984) study and 21-28 based on the FSC samples used in the Harnett (2010) research (6, 87).

Auricular Surface

Age estimates from the auricular surface can be broad, and the mean ages for some of the methods do not differ significantly between each of the phases. However, since the auricular surface changes in a regular manner throughout life, it can be argued that it is more reliable than the pubic symphyses (101). For a comprehensive estimate, the Lovejoy et al. (1985) and the Chamberlain and Buckberry (2002) methods were both applied to the left and right auricular surfaces (102, 103). The later method is often regarded as the more accurate method because it uses a scoring system rather than just phase descriptions (104).

Topography of the auricular surface was observed and cross-referenced with the eight phase descriptions provided by Lovejoy et al. (1985) (103). Since striae were still faintly present on the superior demi-face as well as smooth granularity, the individual placed within phase 3 for the left and right, suggesting an age range of 30 to 34 years of age (Photo 13). Additionally, minimal retro-auricular activity was present, and the individual exhibited little to no apical changes. Moreover, a scoring method was used based on five characteristics: transverse organization (3), surface texture (4), microporosity (2), macroporosity (1), and apical changes (2) (102). With a combined score of 12, the associated stage is stage IV, which provides an estimated age range of 37 to 65 years of age and a mean age of approximately 51 years old. Combining all the results for age estimation, the overall age range of the individual is 20 to 40 years old with a most likely range of 25 to 35 years of age.

Ancestry

Mitochondrial DNA

The Miseq results from Galaxy and Haplogrep are provided in Table 1 which includes data for the following categories: percent endogenous reads (total mapped unique reads), average read length (fragment length measured in base pairs), depth of reads (number of times each base pair was sequenced), percent of reference sequenced covered >1x and >2x (coverage of the base pairs used for haplogroup assignment), variant sites with 1x and >1x coverage (sites that vary from the reference that are only sequenced once and the ones sequenced more than once), and the haplogroup result. Sequencing results show a 179X read depth with a 100 percent coverage. Fragment misincorporation plots, or damage plots, are also provided for the forensic sample and control to indicate the degree of degradation which correlates with the age of the samples. The modernity can be loosely approximated based on the degree of damage represented in these plots. The damage plot for sample BCC #20-100 depicts a red line (C→T substitutions) and a blue line (G→A substitutions) that curve slightly at the ends while laying relatively flat in the center of the plot (Figure 7). The degree of curvature at the ends of these lines indicated the level of damage to the DNA, with larger curves representing more degraded samples in comparison to the reference, and flatter line representing fewer degraded bases (105). The present curvature does indicate the DNA was damaged but not to the extremes that would indicate the antiquity of the skeleton is ancient. Figure 8 depicts the damage plot for the negative control sample. The horizontal lines intermittently interrupted by spikes in the map indicate the presence of trace amounts of DNA. This suggests sample contamination from short fragments of DNA did occur but only to a slight degree, which is to be expected.

Additionally, results indicated the individual belonged to the haplotype J1c3f. The haplogroup J it is most frequently found in Europe (106). However, the J haplogroup has been shown to have some frequency (12%) in the Near East. The most common hypothesis is that, like most European haplogroups, the J haplogroup originated in the Near East and was brought to Europe by the first farm-herding societies during the Neolithic period (107). Geographic origins of the main mtDNA haplogroup based on Mancuso et al. (2008) places the J haplogroup in Western Europe as depicted in Figure 2 (48). Overall, the mtDNA results indicate a European maternal ancestry for the individual based on the geographic frequency of the J haplogroup. Paternal ancestry is not accounted for in this analysis and could be distinct.

Non-Metric Cranial Assessment

Observed non-metric craniofacial traits include a medium nasal spine, moderate nasal aperture width, absence of a post-bregmatic depression, an angled zygomaticomaxillary suture, and wide mastoid form. In reference to the Gill (1986) chart, the individual matched the most with trait descriptions of Eastern Asians, Polynesians, and American Indians. Not all features in this chart were assessed. Ambiguous and damaged features were excluded. As presented in Figure 9, cranial trait scores analyzed based on the Hefner (2009) method showed a higher probability of American Indian (.4) ancestry followed closely by Asian (.32) and then European (.22). Mitochondrial DNA analysis and skeletal based methods show a mixture of European and Asian ancestry.

FORDISC 3.0

After excluding measurements with high deviations and the least likely reference populations, the final calculations were based on 17 measurements and 5 reference groups

(White males, Chinese males, Black males, Vietnamese males, and Guatemalan males). The results indicated the individual was most similar to Chinese males with a posterior probability of .785 and typicality of .013 (Figure 10). White males were the next closest population match but had a significantly lower posterior probability of .148.

Each of the methods for ancestry estimation had differing results, but overall, showed a mix of European and Asian characteristics. Considering the remains were used as an anatomical specimen and the history of anatomical specimens as mentioned above, it is likely that the individual was from India.

Stature

Trotter (1970) Equations

Calculations from the European male equations for the radius, femur, and fibula provided an overall range of 155.8 to 167.5 cm, which is equivalent to a range of 5'1" to 5'6". Results based on East Asian males gave an estimated range of 154.9-169.3 cm (5'1" to 5'6"). The overall stature range per this method is 5'6".

FORDISC 3.0

Similar to the Trotter (1970) method, specific measurements from the ulna, and tibia were excluded. Two measurements from the ossa coxae, pelvic height, and ischial length, were also excluded due to damage on the ischial tuberosities. Results from the Fordisc 3.0 analysis (Figure 11) indicated an estimated stature between 61.3 to 66.7 inches (5'1" to 5'6"). The short regression formula for the femur and fibula provided an estimate of 5'4" with a standard deviation of 2.2", which corresponds with an approximated range of 5'1" to 5'6". Per the Fordisc 3.0 results, the overall estimated stature for the individual is between 5'1" to 5'6".

Trauma and Pathology

The majority of trauma present on the skeleton is due to post-mortem events, including trauma resulting from articulation of the skeleton, normal wear from use as an anatomical specimen, exposure to fluctuation temperatures, and the disarticulation process. A hanging hole is present and located slightly anterior to the bregma (Photo 14). Other drill/bolt holes are present on the glenoid fossas, sacrum, and ossa coxae. The maxilla and mandible exhibit cracking and flaking, plaster and glue is present where someone in the past tried to fix the fracturing areas (Photo 15). The left and right ribs 2 through 6 are fractured vertically along the shafts (Photo 16), and the medial ends of the clavicles (Photo 17). Near the 5th segment, the lateral edges of the sacrum (Photo 18) show minimal signs of damage. As previously mentioned, during the disarticulation process, the posterior wall of the pubic symphyses were damaged.

One area of ante-mortem trauma was noted on the left 11th rib which was identifiable by the presence of a bony callus (Photo 19), indicating healing had begun before time of death (98). No major or identifying pathologies were noted.

Conclusions

A comprehensive forensic case analysis was performed for case BCC #20-100 that employed the use of multiple methods to estimate sex, age, ancestry, and stature in conjunction with associated antemortem and postmortem trauma. Results indicate the individual was likely a male between 25 to 35 years of age with an estimated stature range of 5’1” to 5’6”. Skeletal features show a mix of Asian and European characteristics, and it is likely the individual was from India. No major identifying pathologies were found. The only location of antemortem trauma noted was on the left 11th rib and is identifiable by a bony callus on the midshaft.

Appendix

Table 1. Condensed Galaxy and Haplogrep results.

Sample	% Endogenous reads	Avg. length	% Ref-seq covered >1x	% Ref-seq covered >2x	Variant sites 1x coverage	Variant sites >1x coverage	Mean read depth	Haplogroup
20-100	4.6%	92.64	100%	100%	0	25	178.9915x	J1c3f
Control	10.1%	77.73	18.69%	1.83%	9	0	.2111x	H2a2a1

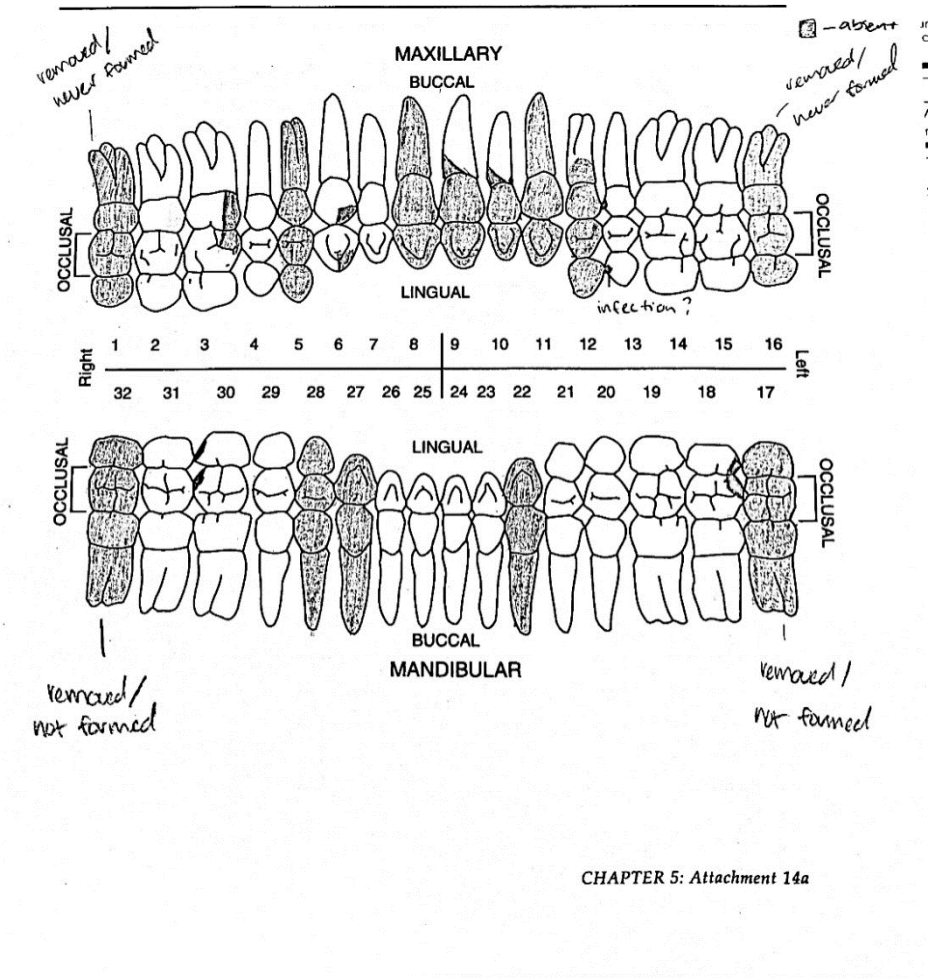

Figure 1. Dental chart illustration. Shaded areas represent absent dentition.

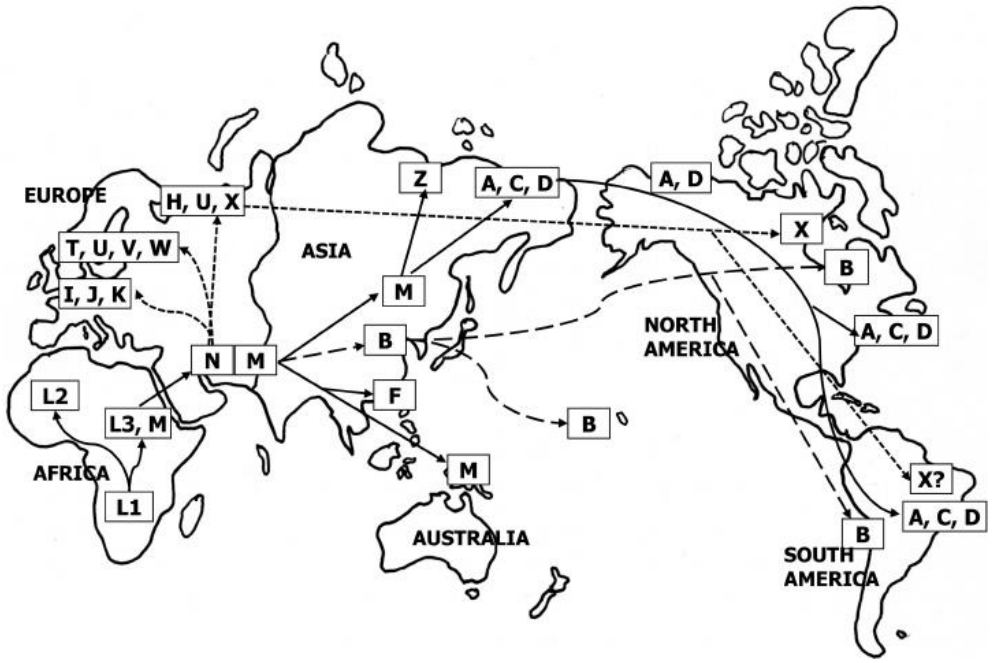

Figure 2. Haplogroup migration routes (Mancuso et al, 2008).

CRANIAL

1.	**GOL** Maximum Cranial Length	176	18.	**DKB** Interorbital Breadth	20
2.	**XCB** Maximum Cranial Breadth	141	19.	**FRC** Frontal Chord	109
3.	**ZYB** Bizygomatic Breadth	117	20.	**PAC** Parietal Chord	106
4.	**BBH** Basion-Bregma Height	122	21.	**OCC** Occipital Chord	92
5.	**BNL** Basion-Nasion Length	95	22.	**FOL** Foramen Magnum Length	37
6.	**BPL** Basion-Prosthion Length	87*	23.	**FOB** Foramen Magnum Breadth	29
7.	**MAB** Maxillo-Alveolar Breadth	55	24.	**MDH** Mastoid Length	22
8.	**MAL** Maxillo-Alveolar Length	46*	25.	**GNI** Chin height	24
9.	**AUB** Biauricular Breadth	114	26.	**HML** Mandibular Body Height	22
10.	**NPH** Upper Facial Height	60*	27.	**TML** Mandibular Body Breadth	10
11.	**WFB** Minimum Frontal Breadth	93	28.	**GOG** Bigonial Width	87
12.	**FMB** Upper Facial Breadth	100	29.	**CDL** Bicondylar Breadth	109
13.	**NLH** Nasal height	N/A	30.	**WRL** Minimum Ramus Breadth	27
14.	**NLB** Nasal Breadth	24	31.	**MRL** Maximum Ramus Breadth	27
15.	**OBB** Orbital Breadth	37	32.	**XRL** Maximum Ramus Height	41
16.	**OBH** Orbital Height	33	33.	**MLT** Mandibular Length	82
17.	**EKB** Biorbital Breadth	98	34.	**MLX** Mandibular Angle	122

Figure 3. Cranial measurements. The asterisks indicate measurements later discarded because of unreliable accuracy due to post-mortem damage.

POSTCRANIAL

		left	right
35.	**Clavicle:** Max. Length	142	141
36.	A-P Diam. Midshaft	10	11
37.	Sup.-Inf. Diam. Midshaft	8	8
38.	**Scapula:** Height	155	151
39.	Breadth	111	109
40.	**Humerus:** Max. Length	303	309
41.	Epicondylar Breadth	50	50
42.	Vertical Diam. Head	41	41
43.	Max. Diam. Midshaft	19	19
44.	Min. Diam. Midshaft	15	15
45.	**Radius:** Max. Length	219	218
46.	Ant.-Post. Diam. Midshaft	10	10
47.	Med.-Lat. Diam. Midshaft	13	14
48.	**Ulna:** Max. Length	236	238
49.	A-P Diameter	14	15
50.	M-L Diameter	10	11
51.	Physiological Length	211*	208*
52.	Min. Circumference	9	10
53.	**Sacrum:** Anterior Length	132	
54.	Anterior Superior Breadth	100	
55.	Max. Trans. Diam. Base	47	
56.	**Pelvis:** Height	x	x
57.	Iliac Breadth	144	143
58.	Pubis Length	80*	77*
59.	Ischium Length	x	x

		left	right
60.	**Femur:** Max. Length	432	433
61.	Bicondylar Length	427	427
62.	Epicondylar Breadth	73	75
63.	Max. Diam. Head	42	42
64.	A-P Subtroch. Diam.	25	25
65.	M-L Subtroch. Diam.	30	29
66.	A-P Midshaft Diam.	25	25
67.	M-L Midshaft Diam.	26	25
68.	Midshaft Circumference	84	83
69.	**Tibia:** Max. Length	x	x
70.	Max. Prox.Epiph. Breadth	65	65
71.	Max. Distal Epiph. Breadth	46	46
72.	Max. Diam. Nutrient For.	28	30
73.	M-L Diam. Nutrient For.	20	23
74.	Circ. Nutrient Foramen	80	83
75.	**Fibula:** Max. Length	326	330
76.	Max. Diameter Midshaft	11	11
77.	**Calcaneus:** Max. Length	55	57
78.	Middle Breadth	41	41
79.	**Sternum:** Length Mesostern.		
80.	Max. Breadth 1st		

Figure 4. Post-cranial measurements. The asterisks indicate measurements later discarded because of unreliable accuracy due to post-mortem damage.

Scores:

Sub-Pub Conc	Med Isch Pub Ram	Vent Arc
4	4	4

Linear Discriminant Functions (unpublished)

score	sex	prob M	prob F	accuracy	vars
-5.182	**MALE**	0.99	0.01	92 / 97	MV
-6.811	**MALE**	1.00	0.00	89 / 98	SMV
-6.376	**MALE**	1.00	0.00	88 / 98	SV
-5.1	**MALE**	0.99	0.01	87 / 96	SM

Logistic regression equation

3.74	**MALE**	**0.98**	**0.02**	98 / 74	SMV

Figure 5. Klales et al. (2012) os coxa sex estimation trait scores and results.

Sex estimation from Walker (2008)

Table 9. Logistic Regression Equations

Scores:

nuchal	mastoid	orbit	glabella	mental
3	3	4	3	4

Sex estimations:

score	sex	prob Male	prob F	accuracy	vars
-3.152	**MALE**	0.96	0.04	88 / 86	gl-ma-me
-1.647	**MALE**	0.84	0.16	85 / 83	gl-ma
-3.143	**MALE**	0.96	0.04	87 / 82	gl-me
-3.379	**MALE**	0.97	0.03	70 / 84	me-ma
-5.41	**MALE**	1.00	0.00	78 /78	or-me
-1.448	**MALE**	0.81	0.19	77 / 83	nu-ma

Figure 6. Walker (2008) cranial sex estimation trait scores and results.

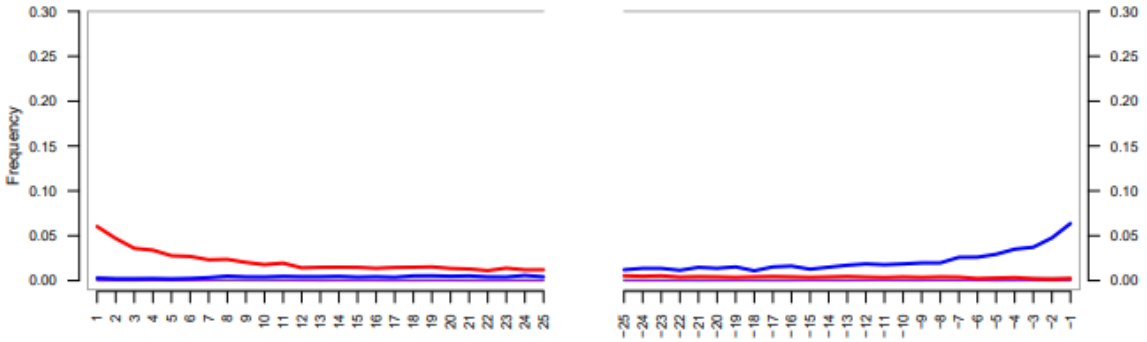

Figure 7. Fragment misincorporation plot for BCC #20-100.

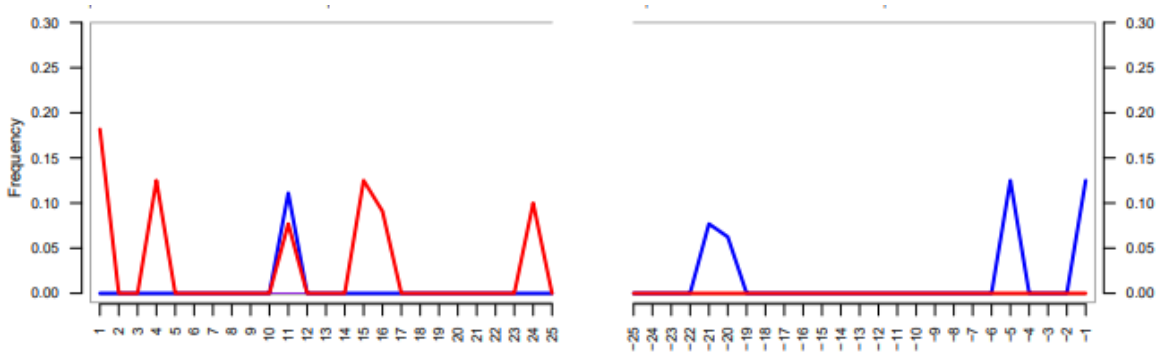

Figure 8. Fragment misincorporation plot for the negative control.

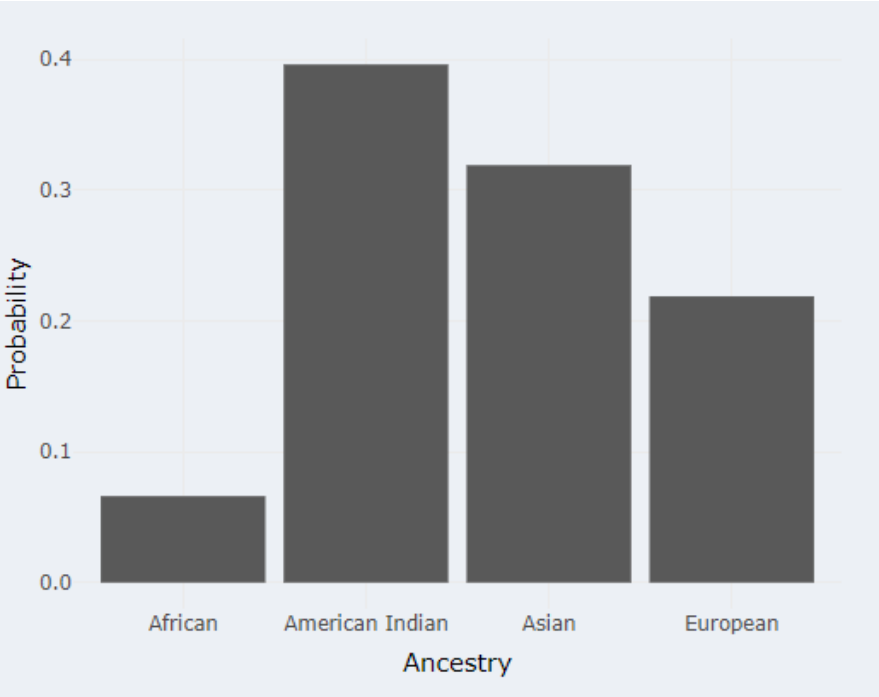

Figure 9. Hefner (2009) cranial ancestry estimation results. Probability outputs from left to right: .07, .40, .32, .22.

Natural Log of VCVM Determinant = 40.1236

Classification Table

From Group	Total Number	Into Group (counts) BM	CHM	GTM	VM	WM	Correct
BM	110	83	6	9	2	10	75.5 %
CHM	74	5	54	1	10	4	73.0 %
GTM	74	3	2	62	7	0	83.8 %
VM	48	0	4	4	40	0	83.3 %
WM	297	19	15	4	5	254	85.5 %

Total Correct: 493 out of 603 (81.8 %) *** CROSS-VALIDATED ***

Multigroup Classification of Current Case

Group	Classified into	Distance from	Probabilities Posterior	Typ F	Typ Chi	Typ R
CHM	**CHM**	34.4	0.785	**0.013**	0.007	**0.013 (74/75)**
WM		37.8	0.148	0.005	0.003	0.007 (296/298)
VM		40.5	0.037	0.003	0.001	**0.020 (48/49)**
BM		41.1	0.028	0.002	0.001	0.009 (110/111)
GTM		46.2	0.002	0.000	0.000	**0.013 (74/75)**

Current Case is closest to CHMs

Figure 10. Fordisc 3.0 ancestry estimation results based on cranial metrics.

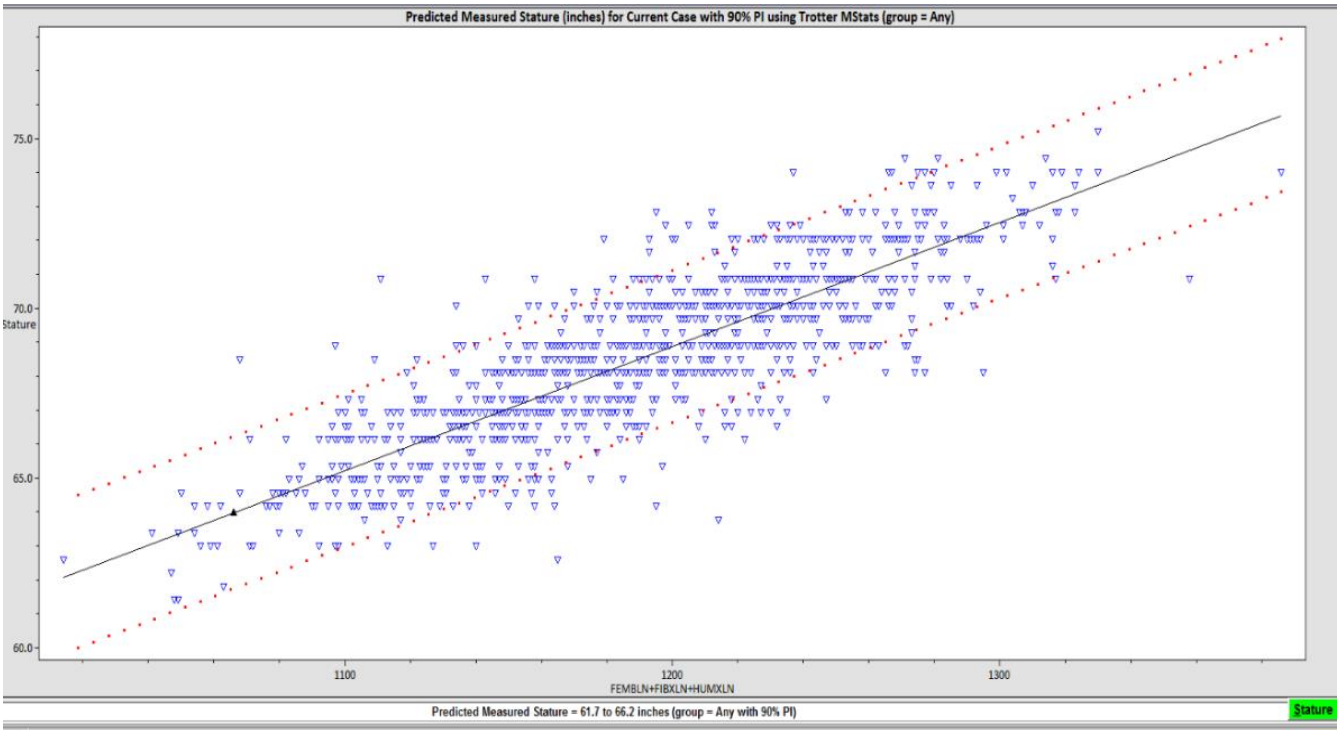

Figure 11. Fordisc 3.0 stature estimation results based on post-cranial measurements. Trotter M Stats were used as reference with a 95% confidence interval.

Photo 1. Remains of BCC #20-100 as received by the Bonner County coroner.

Photo 2. Anterior view of the sternum with part of the remaining cartilage.

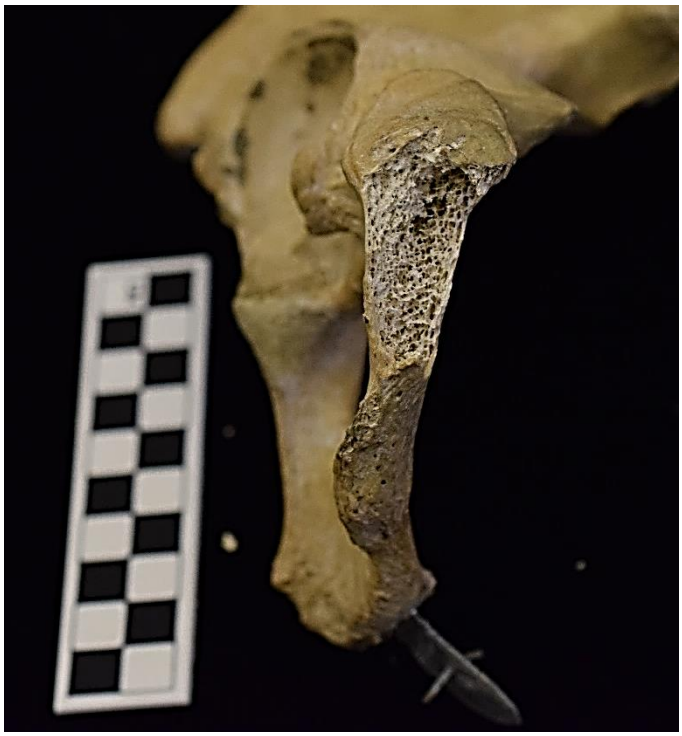
Photo 3. Post-mortem damage to the left ischial tuberosity.

Photo 4. Post-mortem damage to the right ischial tuberosity.

Photo 5. Mid-disarticulation process of the spinal column and pelvic girdle.

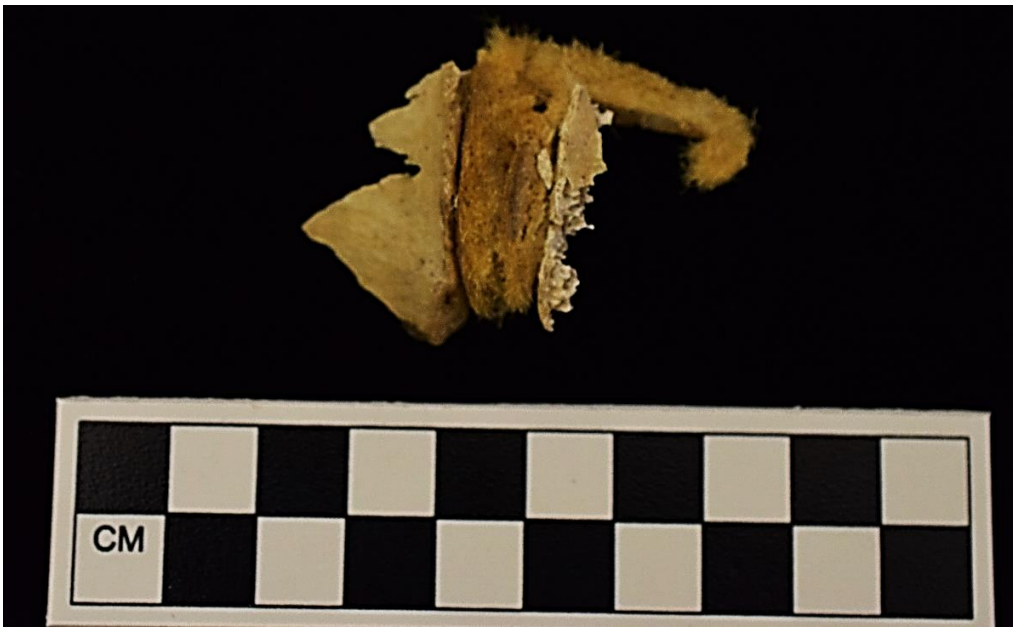

Photo 6. Posterior wall of the pubic symphyses that broke off during disarticulation.

Photo 7. Articulated left humerus and ulna from posterior view.

Photo 8. Articulated left patella, tibia, and talus from anterior view.

Photo 9. Maxillary dentition.

Photo 10. Mandibular dentition.

Photo 11. Sternal end of the left 4th rib.

Photo 12. Sternal end of the right 4th rib.

Photo 13. Right auricular surface.

Photo 14. Hanging hole on the superior portion of the frontal bone, slightly anterior to bregma.

Photo 15. Cracking on the left side of the mandibular body.

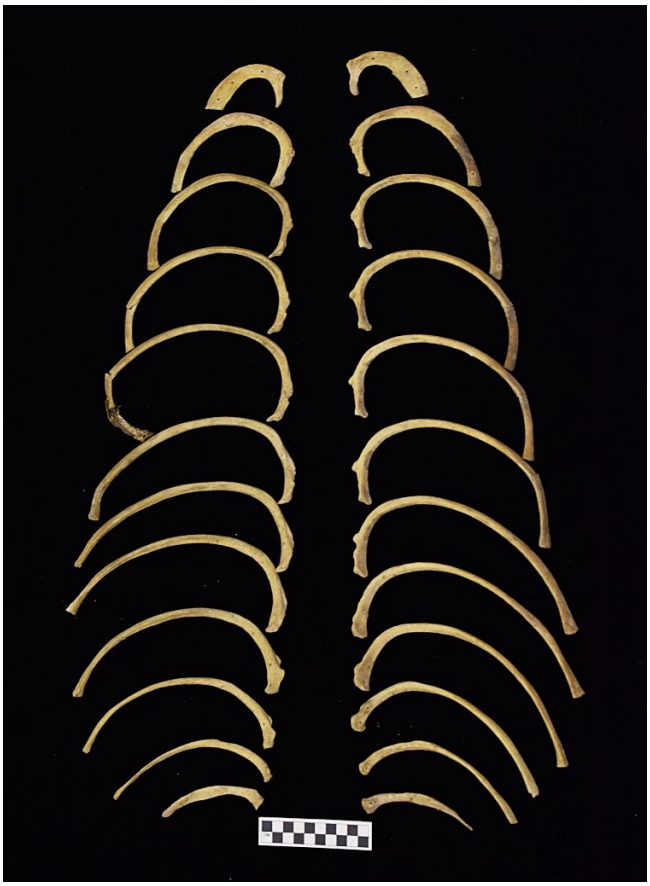
Photo 16. Ribs laid out in anatomical position.

Photo 17. Left clavicle with slight post-mortem damage to the lateral end.

Photo 18. Anterior view of the sacrum.

Photo 19. Ante-mortem fracture healing on the left 11th rib shaft.

References

1. Krogman W. A guide to the identification of human skeletal material. *FBI Law Enforc Bullet.* 1939; 8(8): 3–31.
2. Wiersema JM. Evolution of forensic anthropological methods of identification. Acad Forensic Pathol 2016;6(3):361–9.
3. Spradley MK. Metric methods for the biological profile in forensic anthropology: Sex, ancestry, and stature. Acad Forensic Pathol 2016;6(3):391–9.
4. Marado L, Ribeiro J. Biological profile estimation based on footprints and shoeprints from Bracara Augusta figlinae (brick workshops). Heritage 2018;1(1):33–44.
5. National Research Council. Strengthening forensic science in the United States: a path forward. Washington: National Academies Press 2009; 352.
6. Hartnett KM. Analysis of age-at-death estimation using data from a new, modern autopsy sample--part II: sternal end of the fourth rib: Age-at-death estimation using the fourth rib. J Forensic Sci 2010;55(5):1152–6.
7. Hughes CE, Juarez CA, Hughes TL, Galloway A, Fowler G, Chacon S. A simulation for exploring the effects of the "trait list" method's subjectivity on consistency and accuracy of ancestry estimations: Exploring the effects of the "trait list" method's subjectivity. J Forensic Sci 2011;56(5):1094–106.
8. Urbanová P, Ross AH, Jurda M, Nogueira M-I. Testing the reliability of software tools in sex and ancestry estimation in a multi-ancestral Brazilian sample. Leg Med (Tokyo) 2014;16(5):264–73.
9. Klales AR, Kenyhercz MW. Morphological assessment of ancestry using cranial macromorphoscopics. J Forensic Sci 2015;60(1):13–20.

10. Ubelaker DH, Khosrowshahi H. Estimation of age in forensic anthropology: historical perspective and recent methodological advances. Forensic Sci Res 2019;4(1):1–9.
11. Brothwell DR. Digging up bones. 3rd ed. London, England: Oxford University Press, 1982.
12. Lovejoy CO. Dental wear in the Libben population: its functional pattern and role in the determination of adult skeletal age at death. Am J Phys Anthropol 1985;68(1):47–56.
13. Cooper RN, Fogel RW. The Escape from hunger and premature death, 1700-2100: Europe, America, and the third world. Foreign Aff 2004;83(5):168.
14. Wescott DJ, Zephro LR. Secular change in the femur diaphyseal biomechanical properties of American whites. Hum Biol 2016;88(1):38–46.
15. Sandercock G, Voss C, McConnell D, Rayner P. Ten year secular declines in the cardiorespiratory fitness of affluent English children are largely independent of changes in body mass index. Arch Dis Child 2010;95(1):46–7.
16. Biro FM, Greenspan LC, Galvez MP. Puberty in girls of the 21st century. J Pediatr Adolesc Gynecol 2012;25(5):289–94.
17. Ubelaker DH, Volk CG. A test of the phenice method for the estimation of sex. J Forensic Sci 2002;47(1):19–24.
18. Elliott M, Collard M. FORDISC and the determination of ancestry from cranial measurements. Biol Lett 2009;5(6):849–52.
19. Guyomarc'h P, Bruzek J. Accuracy and reliability in sex determination from skulls: a comparison of Fordisc® 3.0 and the discriminant function analysis. Forensic Sci Int 2011;208(1–3):180.e1-6.
20. Ramsthaler F, Kreutz K, Verhoff MA. Accuracy of metric sex analysis of skeletal remains using Fordisc based on a recent skull collection. Int J Legal Med 2007;121(6):477–82.

21. Hughes CE, Dudzik B, Algee-Hewitt BFB, Jones A, Anderson BE. Understanding (mis)classification trends of Latin Americans in Fordisc 3.1: Incorporating cranial morphology, microgeographic origin, and admixture proportions for interpretation. J Forensic Sci 2019;64(2):353–66.
22. Dunn RR, Spiros MC, Kamnikar KR, Plemons AM, Hefner JT. Ancestry estimation in forensic anthropology: A review. WIREs Forensic Sci 2020;2(4):e1369.
23. Guo G, Fu Y, Lee H, Cai T, Mullan Harris K, Li Y. Genetic bio-ancestry and social construction of racial classification in social surveys in the contemporary United States. Demography 2014;51(1):141–72.
24. Frudakis TN. Ancestry and Admixture. Molecular Photofitting. Elsevier, 2008;35–55.
25. Wagner JK, Yu J-H, Ifekwunigwe JO, Harrell TM, Bamshad MJ, Royal CD. Anthropologists' views on race, ancestry, and genetics: WAGNER et al. Am J Phys Anthropol 2017;162(2):318–27.
26. Michael A, Bengtson J, Blatt S. Genes, race, ancestry, and identity in forensic anthropology: Historical perspectives and contemporary concerns. Forensic Genomics 2021;1(2):41–6.
27. Maier C, Craig A, Adams DM. Language use in ancestry research and estimation. J Forensic Sci 2021;66(1):11–24.
28. Cunha E, Ubelaker DH. Evaluation of ancestry from human skeletal remains: a concise review. Forensic Sci Res 2020;5(2):89–97.
29. Winburn AP, Algee-Hewitt B. Evaluating population affinity estimates in forensic anthropology: Insights from the forensic anthropology database for assessing methods accuracy (FADAMA). J Forensic Sci 2021;66(4):1210–9.

30. Schall JL, Rogers TL, Deschamps-Braly JC. Breaking the binary: The identification of trans-women in forensic anthropology. Forensic Sci Int 2020;309(110220):110220.
31. Garofalo EM, Garvin HM. The confusion between biological sex and gender and potential implications of misinterpretations. Sex Estimation of the Human Skeleton. Elsevier, 2020;35–52.
32. Scheuer L, Black S. Developmental Juvenile Osteology. Academic Press, 2014.
33. Kleisner K, Tureček P, Roberts SC, Havlíček J, Valentova JV, Akoko RM, et al. How and why patterns of sexual dimorphism in human faces vary across the world. Sci Rep 2021;11(1):5978.
34. Dudzik B. Examining cranial morphology of Asian and Hispanic populations using geometric morphometrics for ancestry estimation. Forensic anthropol 2019;2(4). https://doi.org/10.5744/fa.2019.1022.
35. Nass MM, Nass S. Intramitochondrial fibers with DNA characteristics. I. Fixation and electron staining reactions. J Cell Biol 1963;19(3):593–611.
36. Amorim A, Fernandes T, Taveira N. Mitochondrial DNA in human identification: a review. PeerJ 2019;7(e7314):e7314.
37. Chiaroni D, Chiesa V, Frattini F. Investigating the adoption of open innovation in the bio‐pharmaceutical industry: A framework and an empirical analysis. Eur J Innov Manag 2009;12(3):285−305.
38. Salas A, Lareu V, Calafell F, Bertranpetit J, Carracedo A. mtDNA hypervariable region II (HVII) sequences in human evolution studies. Eur J Hum Genet 2000;8(12):964–74.
39. Andrews RM, Kubacka I, Chinnery PF, Lightowlers RN, Turnbull DM, Howell N. Reanalysis and revision of the Cambridge reference sequence for human mitochondrial DNA. Nat Genet 1999;23(2):147.

40. Merheb M, Matar R, Hodeify R, Siddiqui SS, Vazhappilly CG, Marton J, et al. Mitochondrial DNA, a powerful tool to decipher ancient human civilization from domestication to music, and to uncover historical murder cases. Cells 2019;8(5):433.
41. Nahar Sultana GN. Medicolegal aspects and examination techniques in exhumation cases with alleged human rights violation. J forensic sci crim investig 2018;9(1). https://doi.org/10.19080/jfsci.2018.09.555755.
42. Stoneking M, Hedgecock D, Higuchi RG, Vigilant L, Erlich HA. Population variation of human mtDNA control region sequences detected by enzymatic amplification and sequence-specific oligonucleotide probes. Am J Hum Genet 1991;48(2):370–82.
43. Parsons TJ, Coble MD. Increasing the forensic discrimination of mitochondrial DNA testing through analysis of the entire mitochondrial DNA genome. Croat Med J 2001;42(3):304–9.
44. Just RS, Irwin JA, O'Callaghan JE, Saunier JL, Coble MD, Vallone PM, et al. Toward increased utility of mtDNA in forensic identifications. Forensic Sci Int 2004;146 Suppl:S147-9.
45. Mitchell SL, Goodloe R, Brown-Gentry K, Pendergrass SA, Murdock DG, Crawford DC. Characterization of mitochondrial haplogroups in a large population-based sample from the United States. Hum Genet 2014;133(7):861–8.
46. Chinnery PF, Gomez-Duran A. Oldies but goldies mtDNA population variants and neurodegenerative diseases. Front Neurosci 2018;12:682.
47. Gandini F, Achilli A, Pala M, Bodner M, Brandini S, Huber G, et al. Mapping human dispersals into the Horn of Africa from Arabian Ice Age refugia using mitogenomes. Sci Rep 2016;6:25472.
48. Mancuso M, Filosto M, Orsucci D, Siciliano G. Mitochondrial DNA sequence variation and neurodegeneration. Hum Genomics 2008;3(1):71–8.

49. van Oven M, Kayser M. Updated comprehensive phylogenetic tree of global human mitochondrial DNA variation. Hum Mutat 2009;30(2):E386-94.
50. Duong NT, Macholdt E, Ton ND, Arias L, Schröder R, Van Phong N, et al. Complete human mtDNA genome sequences from Vietnam and the phylogeography of Mainland Southeast Asia. Sci Rep 2018;8(1). https://doi.org/10.1038/s41598-018-29989-0.
51. Ma J, Coarfa C, Qin X, Bonnen PE, Milosavljevic A, Versalovic J, et al. mtDNA haplogroup and single nucleotide polymorphisms structure human microbiome communities. BMC Genomics 2014;15(1):257.
52. Habbal O. The Science of Anatomy: A historical timeline. Sultan Qaboos Univ Med J 2017;17(1):e18–22.
53. Guerrini A. Duverney's skeletons. Isis 2003;94(4):577–603.
54. Carney S. The Red Market. Mai Tian/Tsai Fong Books, 2012.
55. Davies C. Dirt, death, decay and dissolution: American denial and British avoidance. Contemporary Issues in the Sociology of Death, Dying and Disposal. London: Palgrave Macmillan UK, 1996;60–71
56. Byock A. Embalming the American body: Sentimental mourning on the cusp of the civil war. Dying and Death. BRILL, 2007;xiii–16.
57. Troyer J. Embalmed vision. Mortality (Abingdon) 2007;12(1):22–47.
58. Cumback K. A bone to pick with international law: The ghoulish trade in human remains. 2018.
59. Lalwani R, Kotgirwar S, Athavale SA. Changing medical education scenario: a wakeup call for reforms in Anatomy Act. BMC Med Ethics 2020;21(1):63.
60. Davidson K, Graham S, Huffer D. Exploring Taste Formation and Performance in the Illicit Trade of Human Remains on Instagram. Springer, 2021.

61. Gordon RM. The infamous Burke and hare: Serial killers and resurrectionists of nineteenth century Edinburgh. Jefferson, NC: McFarland, 2009.
62. No. 17866. Agreement on the transfer of corpses. Concluded at Strasbourg on 26 October 1973. United Nations Treaty Series. UN, 1998;382–382.
63. Bruzek J, Murail P. Methodology and reliability of sex determination from the skeleton. Forensic Anthropology and Medicine. Totowa, NJ: Humana Press, 2007;225–42.
64. Betti L. Sexual dimorphism in the size and shape of the os coxae and the effects of microevolutionary processes: Sexual Dimorphism in Pelvic Size and Shape. Am J Phys Anthropol 2014;153(2):167–77.
65. González N, Rascón Pérez J, Chamero B, Cambra-Moo O, González Martín A. Geometric morphometrics reveals restrictions on the shape of the female os coxae. J Anat 2017;230(1):66–74.
66. Phenice TW. A newly developed visual method of sexing the os pubis. Am J Phys Anthropol 1969;30(2):297–301.
67. Sutherland LD, Suchey JM. Use of the ventral arc in pubic sex determination. J Forensic Sci 1991;36(2):501–11.
68. Rogers T, Saunders S. Accuracy of sex determination using morphological traits of the human pelvis. J Forensic Sci 1994;39(4):1047–56.
69. Bruzek J. A method for visual determination of sex, using the human hip bone. Am J Phys Anthropol 2002;117(2):157–68.
70. Klales AR, Ousley SD, Vollner JM. A revised method of sexing the human innominate using Phenice's nonmetric traits and statistical methods. Am J Phys Anthropol 2012;149(1):104–14.

71. Berrizbeitia EL. Sex determination with the head of the radius. J Forensic Sci 1989;34(5):1206–13.
72. France DL. Observational and metric analysis of sex in the skeleton. In: Reichs KJ, editor. Springfield, IL: Charles C. Thomas, 1998;163–86.
73. Albanese J, Eklics G, Tuck A. A metric method for sex determination using the proximal femur and fragmentary hipbone. J Forensic Sci 2008;53(6):1283–8.
74. Spradley MK, Jantz RL. Sex estimation in forensic anthropology: skull versus postcranial elements: Sex estimation in forensic anthropology. J
75. Rogers TL. A visual method of determining the sex of skeletal remains using the distal humerus. J Forensic Sci 1999;44(1):57–60.
76. Pozzi A, Raffone C, Belcastro MG, Camilleri-Carter TL. Sex estimation in cranial remains: A comparison of machine learning and discriminant analysis in Italian populations. bioRxiv. 2020.
77. Durić M, Rakocević Z, Donić D. The reliability of sex determination of skeletons from forensic context in the Balkans. Forensic Sci Int 2005;147(2–3):159–64.
78. Walker PL. Sexing skulls using discriminant function analysis of visually assessed traits. Am J Phys Anthropol 2008;136(1):39–50.
79. Buikstra J, Ubelaker D. Standards for data collection from human skeletal remains. Am J Hum Biol 1994;7(5):672–672.
80. Cardoso HFV. Age estimation of adolescent and young adult male and female skeletons II, epiphyseal union at the upper limb and scapular girdle in a modern Portuguese skeletal sample. Am J Phys Anthropol 2008;137(1):97–105.
81. Franklin D. Forensic age estimation in human skeletal remains: current concepts and future directions. Leg Med (Tokyo) 2010;12(1):1–7.

82. Cunningham C, Scheuer L, Black S. Skeletal Development and Ageing. Developmental Juvenile Osteology. Elsevier, 2016;5–18.
83. McKern T, Stewart T.. Skeletal age changes in young American males, analyzed from the standpoint of age identification. Technical report EP-45, environmental protection research division, quartermaster research and development center, U.s. army, Natick, 1957. Viii + 179 pp., 87 figs., 52 tables. Am Antiq 1957;24(2):198–9.
84. Verma M, Verma N, Sharma R, Sharma A. Dental age estimation methods in adult dentitions: An overview. J Forensic Dent Sci 2019;11(2):57–63.
85. White TD, Black MT, Folkens PA. Human Osteology. 3rd ed. San Diego, CA: Academic Press, 2011.
86. Yoder C, Ubelaker DH, Powell JF. Examination of variation in sternal rib end morphology relevant to age assessment. J Forensic Sci 2001;46(2):223–7.
87. Işcan MY, Loth SR, Wright RK. Metamorphosis at the sternal rib end: a new method to estimate age at death in white males. Am J Phys Anthropol 1984;65(2):147–56.
88. Meena M, Rani Y, Rani M. Bilateral metamorphological variation at sternal end of fourth rib. Eurasian Journal of Anthropology 2013;3(2):41–6.
89. Pinhasi R, Fernandes DM, Sirak K, Cheronet O. Isolating the human cochlea to generate bone powder for ancient DNA analysis. Nat Protoc 2019;14(4):1194–205.
90. Dabney J, Knapp M, Glocke I, Gansauge M-T, Weihmann A, Nickel B, et al. Complete mitochondrial genome sequence of a Middle Pleistocene cave bear reconstructed from ultrashort DNA fragments. Proc Natl Acad Sci U S A 2013;110(39):15758–63.
91. Meyer M, Kircher M. Illumina sequencing library preparation for highly multiplexed target capture and sequencing. Cold Spring Harb Protoc 2010;2010(6):db.prot5448.

92. Weissensteiner H, Pacher D, Kloss-Brandstätter A, Forer L, Specht G, Bandelt H-J, et al. HaploGrep 2: mitochondrial haplogroup classification in the era of high-throughput sequencing. Nucleic Acids Res 2016;44(W1):W58–63.

93. Gill G, Rhine S. Skeletal Attribution of Race: Methods for Forensic Anthropology. Albuquerque, New Mexico: Maxwell Museum of Anthropology 1990.

94. Hefner JT. Cranial nonmetric variation and estimating ancestry. J Forensic Sci 2009;54(5):985–95.

95. Jantz R. L., Ousley S. D. Fordisc, *version 3.0.* Knoxville, TN: University of Tennessee 2005.

96. Trotter M, Gleser GC. Estimation of stature from long bones of American Whites and Negroes. Am J Phys Anthropol 1952;10(4):463–514.

97. Ismail NA, Abu Bakar SN, Abdullah N, Shafie MS, Mohd Nor F. Stature estimation in the South-East Asian population: A systematic review. Malays J Pathol 2019;41(2):83–9.

98. Blackwell W. Skeletal trauma analysis: Case studies in context. 1st ed. Nashville, TN: John Wiley & Sons, 2015.

99. White TD, Folkens PA. The Human Bone Manual. San Diego, CA: Academic Press, 2005.

100. Ortner DJ. Identification of pathological conditions in human skeletal remains. 2nd ed. San Diego, CA: Academic Press, 2003.

101. Osborne DL, Simmons TL, Nawrocki SP. Reconsidering the auricular surface as an indicator of age at death. J Forensic Sci 2004;49(5):905–11.

102. Buckberry JL, Chamberlain AT. Age estimation from the auricular surface of the ilium: a revised method. Am J Phys Anthropol 2002;119(3):231–9.

103. Lovejoy CO, Meindl RS, Pryzbeck TR, Mensforth RP. Chronological metamorphosis of the auricular surface of the ilium: a new method for the determination of adult skeletal age at death. Am J Phys Anthropol 1985;68(1):15–28.

104. Priya E. Methods of skeletal age estimation used by forensic anthropologists in adults: A review. Foresic Res Criminol Int J 2017;4(2). https://doi.org/10.15406/frcij.2017.04.00104.

105. Sullivan AP, Marciniak S, O'Dea A, Wake TA, Perry GH. Modern, archaeological, and paleontological DNA analysis of a human-harvested marine gastropod (Strombus pugilis) from Caribbean Panama. bioRxiv. 2020.

106. Fernandes V, Triska P, Pereira JB, Alshamali F, Rito T, Machado A, et al. Genetic stratigraphy of key demographic events in Arabia. PLoS One 2015;10(3):e0118625.

107. Richards M, Macaulay V, Hickey E, Vega E, Sykes B, Guida V, et al. Tracing European founder lineages in the near eastern mtDNA pool. Am J Hum Genet 2000;67(5):1251–76.